Atmos. Chem. Phys. Discuss., 14, 2021–2042, 2014
www.atmos-chem-phys-discuss.net/14/2021/2014/
doi:10.5194/acpd-14-2021-2014

Atmospheric Chemistry and Physics Discussions

Characterization of OMI tropospheric NO_2 over the Baltic Sea region

I. Ialongo[1], J. Hakkarainen[1], N. Hyttinen[1], J.-P. Jalkanen[2], L. Johansson[2], F. Boersma[3], N. Krotkov[4], and J. Tamminen[1]

[1]Finnish Meteorological Institute, Earth Observation Unit, Helsinki, Finland
[2]Finnish Meteorological Institute, Air Quality Unit, Helsinki, Finland
[3]Royal Netherlands Meteorological Institute, Climate Observations Department, De Bilt, the Netherlands
[4]Laboratory for Atmospheric Chemistry and Dynamics, NASA Goddard Space Flight Center, Greenbelt, Maryland, USA

Received: 6 November 2013 – Accepted: 10 January 2014 – Published: 23 January 2014

Correspondence to: I. Ialongo (iolanda.ialongo@fmi.fi)

Published by Copernicus Publications on behalf of the European Geosciences Union.

Abstract

Satellite-based data are very important for air quality applications in the Baltic Sea area, because they provide information on air pollution over sea and there where ground-based network and aircraft measurements are not available. Both the emissions from urban sites over land and ships over sea, contribute to the tropospheric NO_2 levels. The tropospheric NO_2 monitoring at high latitudes using satellite data is challenging because of the reduced light hours in winter and the snow-covered surface, which make the retrieval complex, and because of the reduced signal due to low Sun.

This work presents a detailed characterization of the tropospheric NO_2 columns focused on part of the Baltic Sea region using the Ozone Monitoring Instrument (OMI) tropospheric NO_2 standard product. Previous works have focused on larger seas and lower latitudes. The results showed that, despite the regional area of interest, it is possible to distinguish the signal from the main coastal cities and from the ships by averaging the data over a seasonal time range. The summertime NO_2 emission and lifetime values ($E = (1.0 \pm 0.1) \times 10^{28}$ molec. and $\tau = (3.0 \pm 0.5)$ h, respectively) in Helsinki were estimated from the decay of the signal with distance from the city center. The method developed for megacities was successfully applied to a smaller scale source, in both size and intensity (i.e., the city of Helsinki), which is located at high latitudes ($\sim 60^{\circ}$ N). The same methodology could be applied to similar scale cities elsewhere, as far as they are relatively isolated from other sources.

The transport by the wind plays an important role in the Baltic Sea area. The NO_2 spatial distribution is mainly determined by the contribution of strong westerly winds, which dominate the wind patterns during summer. The comparison between the emissions from model calculations and OMI NO_2 tropospheric columns confirmed the applicability of satellite data for ship emission monitoring. In particular, both the emission data and the OMI observations showed similar year-to-year variability, with a drop in year 2009, corresponding to the effect of the economical crisis.

ACPD
14, 2021–2042, 2014

1 Introduction

Nitrogen oxides ($NO_x = NO + NO_2$) play an important role in tropospheric chemistry, participating in the ozone and aerosol production processes. NO_x is mainly generated in polluted regions by anthropogenic combustion and it is toxic when present at high concentrations at the surface. An important source of NO_x are also the ship emissions, as they represent a relevant part (3–6 $Tg\,N\,yr^{-1}$) of the global NO_x production (50 $Tg\,N\,yr^{-1}$) (Beirle et al., 2011 and references therein). NO_x ship emissions are the most dominant anthropogenic source in the marine boundary layer (MBL), far away from densely populated coasts; this is particularly important, since the ozone production efficiency is high at the low NO_x concentrations typically occurring in the MBL. The balance between NO and NO_2 depends on the photolysis rate of NO_2.

Satellite-derived tropospheric NO_2 data have been extensively used to monitor air quality over polluted and urban areas (see, e.g., some recent results in Russell et al., 2012; Bechle et al., 2013; David et al., 2013; Ghude et al., 2013; Hilboll et al., 2013; Lamsal et al., 2013). Van der A et al. (2008), for example, estimated the NO_2 trends on global scale using 10 yr of satellite data, identifying the largest increase over East-China. Furthermore, Castellanos and Boersma (2012) observed a reduction in nitrogen oxides over Europe driven by the 2008–2009 economical recession and by the European NO_x emission regulation. Recently, Streets et al. (2013) presented an overview on the current capability of emissions estimation from satellite retrievals.

The tropospheric NO_2 data from several satellite-based instruments showed also the capability to identify the major shipping lanes in the world. Beirle et al. (2004) presented the first detection of ship tracks in NO_2 maps derived from satellite data using GOME (Global Ozone Monitoring Experiment) data, along the shipping lane from Sri Lanka to Indonesia. Richter et al. (2004); Franke et al. (2009) and Marmer et al. (2009) extended the analysis using combined tropospheric NO_2 data from several satellite instruments. The global economic cycle and satellite-derived NO_2 trends over the major international shipping lanes have been recently compared by de Ruyter de Wildt et al. (2012). Vinken

ACPD
14, 2021–2042, 2014

et al. (2013) used the GEOS-Chem model to produce a ship emission inventory based on OMI DOMINO tropospheric NO_2 products, including the Baltic Sea area.

Shipping contributes significantly to the air pollution levels in Europe and the health of coastal populations and the Baltic Sea ecosystem can be affected by increasing emissions from maritime transportation. Corbett et al. (2007) assessed that the shipping-related emissions are responsible for about 60 000 deaths annually and they estimated that, globally, the annual mortalities due to ship pollution could increase by 40 % by 2012. In contrast to the NO_x emissions over land, currently there is no a specific legislation to limit the NO_x emissions from ships. This produced an increase in the shipping emissions estimated by about 3 % per year (Eyring et al., 2010). Therefore, there is a strong need for monitoring the NO_x emissions from ships in the Baltic Sea region, together with the land-derived emissions monitoring. According to the european directives, the so called SO_x and NO_x Emission Control Areas (SECA and NECA) will be implemented in the Baltic Sea and the need for air pollution monitoring will further increase. Recently, anyway, the authorities postponed the application of the NECA rules until 2021.

Satellite-based tropospheric NO_2 columns from the Dutch-Finnish Ozone Monitoring Instrument (OMI), flying onboard NASA's EOS-Aura satellite, became available in 2004 and provide almost daily global coverage with nominal spatial resolution of $13 \times 24\ km^2$ (Boersma et al., 2011; Bucsela et al., 2013). Baltic Sea and its coastal region, however, are challenging; high latitude regions may suffer for missing data because the NO_2 observations with high solar zenith angle or snow/ice surface are not considered reliable and, therefore, excluded from the analysis. The NO_x emissions in the Baltic Sea region are also much smaller than in other more polluted regions, making the signal detection more challenging. Furthermore, being the Baltic Sea area relatively small, the contributions from the different sources (land and marine) can be mixed.

Most of the previous studies on monitoring tropospheric NO_2 from satellite focused on middle-low latitudes (see, e.g., Beirle et al., 2011; de Ruyter de Wildt et al., 2012). Furthermore, the uncertainties on NO_x shipping and city emissions as well as lifetime

ACPD
14, 2021–2042, 2014

estimations remain still large (see e.g., Stavrakou et al., 2013). Thus, it is important to study the tropospheric NO_2 pollution from relatively weak sources located at high latitudes.

This paper will focus on monitoring the tropospheric NO_2 levels over the Baltic Sea region, both over marine and coastal areas. The open sea area and the main coastal cities around 60° N will be considered. The total emission and lifetime will be estimated in Helsinki using OMI NO_2 data and wind information. In addition, the changes in NO_2 levels over the period 2005–2011 will be analysed and compared with the information derived from the ship emission model.

2 Data and methodology

The OMI NO_2 tropospheric columns were used in this work. Two NO_2 products are available from OMI: NASA's standard product (SP) version 2.1 (Bucsela et al., 2013) and KNMI's DOMINO product version 2 (Boersma et al., 2011). Both products share the same slant column derivation based on the DOAS (Differential Optical Absorption Spectroscopy) method, but differ in a way of converting slant columns into the tropospheric vertical columns. The OMI NO2 standard product, SP version 2.1 was considered for this study. The algorithm is described in detail by Bucsela et al. (2013), as well as the initial comparison with DOMINO V2 product and aircraft in situ measurements. Comprehensive validation with independent measurements is on-going study and will be a subject of a separate paper (Lok Lamsal, private communication).

In this work, the tropospheric NO_2 Level 2 data were gridded on $0.1^\circ \times 0.1^\circ$ in latitude and longitude directions and averaged over seasonal time scales. Averaging over many days over a grid box smaller than the instrument pixel size ($13 \times 24\,km^2$), allows to increase the effective spatial resolution (Fioletov et al., 2011). The OMI pixels corresponding to SZA larger than 70° and with effective cloud fraction (OMCLDO2 product) larger than 30 % were removed before gridding the data. The analysis focused on sum-

ACPD
14, 2021–2042, 2014

mer season (1 June–31 August), when more data are available at the latitudes of the Baltic Sea region.

The methodology developed by Beirle et al. (2011) for megacities, was applied to OMI data in the Baltic Sea area. The effect of transport by the wind was analysed using the ECMWF wind mean values at 12:00 UTC below 950 hPa altitude. The daily NO_2 data were gridded taking into account only the pixels where the wind speed (w) is smaller than $5\,m\,s^{-1}$ and analysing separately the different wind directions (from North, South, East and West), once the weak winds were removed. The different wind directions were separated identifying four different sectors around the four cardinal points (from NW to NE, from NE to SE, from SE to SW and from SW to NW).

The NO_2 emission and lifetime parameters in Helsinki were estimated applying a methodology based on the average decay of the signal with the distance from the city center. The westerly winds were taken into account in the analysis, because the largest part of the data is collected under these conditions. The model proposed by Beirle et al. (2011) was used to fit the NO_2 line densities, which were derived integrating the NO_2 data in across-wind direction (i.e., zonally) over 2 latitude degrees interval. The fitting model is the convolution of exponential and Gaussian functions, scaled by the emission factor E and the offset background factor B. The e-folding distance x_0 (i.e., the distance over which the linear density decreases by a factor of e), derived from the fit, was then used to calculate the summer mean lifetime $\tau = x_0/w$, where w is the mean zonal wind speed in the direction from West to East. This lifetime must be considered as a dispersion time, which includes the effects of chemical conversion, wind advection and deposition. Also, the coefficient E is actually a burden parameter, which refers to the total amount of molecules observed near the source. The mathematical notation used here is the same described by Beirle et al. (2011) in the supporting material.

The estimation problem is nonlinear with five parameters to be estimated (total emissions E, e-folding distance x_0, background B, width of the Gaussian convolution function σ and location of the source with respect to city center X). The posterior distribution of these unknown parameters was solved using Markov chain Monte Carlo (MCMC)

ACPD
14, 2021–2042, 2014

sampling method, which is very useful in low-dimensional non-Gaussian problems allowing also the non-linearity to be properly modeled. Non-informative prior distribution was assumed for all the unknown parameters. For the practical implementation of the algorithm the MCMC Toolbox by Laine (2008) was used and the adaptive MCMC algorithms by Haario et al. (2001) and Haario et al. (2006) were found to be easily applicable in this case. The convergence of the MCMC algorithm was ensured by sampling long enough chain (100 000 points). The estimates of the total emission E and e-folding distance x_0 were computed as mean (expectation) values of the posterior distribution and the uncertainty was characterized using the standard deviation of the posterior distribution around the estimate.

The OMI NO_2 tropospheric columns in the marine boundary layer were compared with the NO_x emissions of marine traffic as derived from the STEAM model (Ship Traffic Emission Assessment Model), based on the messages provided by the Automatic Identification System (AIS), which enable the positioning of ships with high spatio-temporal resolution (Jalkanen et al., 2009, 2012).

3 Results

Figure 1 (upper left panel) shows the map over Baltic Sea region of OMI tropospheric NO_2 tropospheric columns averaged over the summer days 2005–2011. The major urban NO_2 sources (marked by their initials and white boxes), i.e., the city of Helsinki (60.2° N, 25.0° E), Saint Petersburg (59.95° N, 30.3° E) and Stockholm (59.3° N, 18.0° E), are visible as red-black spots. In the same panel it is possible to identify the main shipping lane in the Baltic Sea, going from South-West to North-East with higher signal in the central area of Baltic Sea. The focus area (Fig. 1 – white rectangle around the point 57.5° N, 19° E) over the Baltic Sea was selected to minimize the influence of the emissions from land sources. Other regions over sea (i.e. Stockholm–Helsinki lane) were not analysed to avoid the possible influence of urban sources.

ACPD
14, 2021–2042, 2014

Figure 1 (lower left panel) shows the summer mean NO_2 map when the wind speed (w), is smaller than 5 m s^{-1}. The NO_2 values corresponding to the pixels with stronger wind speed were removed in order to highlight the emission sources. In this case, the high NO_2 signal is stronger and it remains closer to the sources; the number of data used in the average is smaller than in the previous case (about 30 % of the total available data). The wind intensity and direction play an important role in determining the tropospheric NO_2 distribution and they will be analysed later in this work. Other features visible from the map are the cities of Tallinn (59.4° N, 24.7° E) and Turku (60.45° N, 22.3° E).

In Fig. 1 (right panel), the 2005–2011 time series of the summer means over the main cities and over Baltic Sea area, are shown under all wind conditions (continuous lines) as well as when strong winds were removed (dashed lines). The analysis was restricted to the summer months as not enough and homogeneously distributed data were available during other seasons. The time series show a local minimum in 2009 in Saint Petersburg and in the Baltic Sea area. A similar local minimum of NO_2 in 2009 was observed by Castellanos and Boersma (2012) for several cities in Europe and by de Ruyter de Wildt et al. (2012) for the major shipping lanes. In both cases, the observed reduction was interpreted as the consequence of the 2008–2009 economical recession, which caused a reduction of the emissions from both urban and ship sources. This behavior is more apparent under weak wind conditions (dashed lines in Fig. 1); the transport by the wind acts to dampen the year-to-year variability in NO_2 tropospheric columns. Helsinki and Stockholm time series remain more flat during the considered period. In particular, a NO_2 decrease from year 2008 to 2009 was observed in Helsinki, but the minimum NO_2 value was observed in 2010, in agreement with previous results (see inset city names in Fig. 6 in Castellanos and Boersma, 2012). Thus, other factors than the anthropogenic sources may have contributed to the NO_2 distribution over Helsinki. Overall, the absolute levels of tropospheric NO_2 are higher for the urban sites (especially Saint Petersburg) and smaller for the central Baltic Sea area.

ACPD
14, 2021–2042, 2014

The wind intensity and direction over the Baltic Sea area were analysed for the main coastal cities and in the central Baltic Sea area. Figure 2 shows the distribution of the wind directions as a polar plot together with the histogram of the wind speed at noon (UTC time) during summer 2005–2011. The wind data over Helsinki and the central Baltic Sea area are shown in the upper and lower panels, respectively (corresponding to the pixels in the white boxes of Fig. 1). The polar plots show that the wind patterns are generally dominated by the westerlies during summer. The histograms follow a logarithmic distribution with peak between 5 and 7.5 $m\,s^{-1}$ in both areas. The fraction of pixels with wind speed below the threshold of 5 $m\,s^{-1}$ is below 35 % in Helsinki and about 25 % in the Baltic Sea area. These percentage were calculated with respect to the total number of pixels included in the area marked by the white boxes (Fig. 1). Thus, the largest part of the pixels is removed when only the weak winds are taken into account, introducing a larger statistical error in the calculation of the mean NO_2 spatial distribution.

Figure 3 illustrates the effect of the different wind directions and speeds on the tropospheric NO_2 distribution around Helsinki area. The central panel in Fig. 3 refers to the pixels where only weak winds were considered ($w < 5\,m\,s^{-1}$); the four surrounding panels correspond to the NO_2 tropospheric columns averaged separately for different wind directions (winds blowing from North, West, South and East, are respectively showed moving clockwise from the top panel). Each grid pixel is associated to one of the wind sectors according to the corresponding ECMWF average wind direction below 950 hPa. The resulting NO_2 spatial patterns clearly show the outflow of NO_2 from Helsinki, consistently with the wind directions, so that when wind blows, for example, from West, the largest NO_2 signal is observed East from the city. Similar results were achieved around the city of Riyadh and other megacities as shown by Beirle et al. (2011). The results shown in Fig. 3 demonstrate that the same methodology can be applied to Helsinki and its surrounding area, which have about 1 million inhabitants.

Figure 4 shows the NO_2 line densities (blue color), sampled using OMI pixels under westerly wind conditions, as a function of the eastward distance to Helsinki. The profile

ACPD
14, 2021–2042, 2014

peak is displaced eastward because of the effect of the air mass transport by the westerly winds. The resulting values for e-folding distance $x_0 = (52 \pm 9)$ km and the emission parameter $E = (1.0 \pm 0.1) \times 10^{28}$ molec. were derived from the mean fitted model (Fig. 4 – black line). The summer mean lifetime value $\tau = (3.0 \pm 0.5)$ h was then estimated by the ratio x_0/w, with $w = (4.9 \pm 0.2)$ m s^{-1}. The errors on the estimated parameters are the standard deviations derived from the MCMC calculations. The error bars in Fig. 4 were calculated using the error propagation for the discrete integral and they do not include the contribution from all the sources of errors: for a complete analysis of the uncertainties see Beirle et al. (2011). The lifetime τ agrees within the error bars (but smaller as absolute value) with the summertime value obtained by Beirle et al. (2011) for Moskow ($\tau \simeq (4 \pm 2)$ h), which is located at about 5 latitude degrees South of Helsinki.

The wind effect was analysed also in the center of the Baltic Sea, where a large NO_2 signal was observed. In this case, the wind conditions are not the only cause of transport of the polluted air, as also the ships, which constitute the main emission source in this region, are moving along the major shipping lane from Denmark to the Finnish Gulf and to Stockholm. The analysis of the number of pixels associated with the different wind directions (not plotted here) confirms that the wind patterns in the Baltic Sea area are dominated by the westerlies, which give the largest contribution to the mean seasonal NO_2 spatial patterns. Figure 5 shows the summer average of NO_2 over the Baltic Sea region when all wind conditions (left panel), weak winds (central panel) and westerly winds only (right panel) are taken into account. The high NO_2 signal in the central Baltic Sea is visible when all wind conditions (left panel) are considered. The signal is also visible when only the weak winds (central panel) are taken into account, even though a smaller amount of data are available under these wind conditions. When only the westerly winds are considered, the NO_2 signal is most visible because a larger number of pixels satisfy the wind-driven condition, thus increasing the signal-to-noise ratio. On the other hand, the NO_2 patterns over sea can be influenced by the air masses transported from the land sources. Thus, the time series analysis was limited to the

ACPD
14, 2021–2042, 2014

central area of the Baltic Sea (the black box in Fig. 6 centred at 57.5° N-19° E), where the minimum mixing between the emissions from land and sea sources is expected.

The seasonal NO_x emissions (Fig. 6 – left panel) from maritime traffic as derived from STEAM model were compared with the tropospheric NO_2 columns (Fig. 6 – central panel) for the period July–August 2006–2011. The analysis was restricted to July and August because of a significant data gap in the NO_x emission data in June 2006 and 2010. No NO_x emission information were available for year 2005. The NO_x emission data (Fig. 6 – left panel) show that the ship emission sources are mostly located along one main shipping lane along the direction from SW to NE, with some secondary branches. The emission patterns correspond to high NO_2 signal observed from OMI data in the central Baltic Sea area (Fig. 6 – central panel). The time series of both NO_x emissions and OMI NO_2 tropospheric columns are shown in the right panel in Fig. 6. The time series follow a similar behaviour, both showing an increase up to 2008 and a decrease in 2009, before slightly increasing again until 2011. The tropospheric NO_2 observed from OMI decreased by about 6×10^{15} molec. cm^{-2} from 2008 to 2009, corresponding to a reduction in the NO_x emissions by about 1.2×10^5 g/month per pixel unit. These results must be analysed considering that the changes in NO_2 tropospheric columns are close to the detection limit for OMI ($\pm 5 \times 10^{14}$ molec. cm^{-2}). Furthermore, the uncertainties related to the calculations from STEAM model depend on both the emission factor and the power level of every single ship. When comparing the model results with the existing emission inventories, the difference is in the order of 10–15 % (Jalkanen et al., 2012).

4 Summary and discussion

In this paper the OMI NO_2 tropospheric columns were used to describe the air pollution levels in the Baltic Sea and its coastal area. Both land (urban sites) and marine (ships) sources were taken into account in the analysis. OMI NO_2 data demonstrated their applicability to detect the signal coming from relatively small emission sources, such as

ACPD
14, 2021–2042, 2014

ships and coastal cities at high latitudes. This is the first time ship and urban emissions have been mapped from space with such detail in this area.

The transport of air masses by the wind plays an important role in defining the spatial distribution of NO_2 in the Baltic Sea area, as demonstrated when the NO_2 data were averaged separately for different wind directions. Reducing the analysis to weak wind conditions ($w < 5\,m\,s^{-1}$) helps in identifying the urban sources, but it reduces by at least 70 % the total number of data available for the seasonal average. When looking at the marine area in the central Baltic Sea, where the ships are the main source of NO_x emission, the NO_2 data corresponding to westerly wind conditions showed to give the largest contribution to the NO_2 spatial patterns. This case corresponds also to the situation with the largest continental outflow. On the other hand, the weak winds correspond to the 25 % of the available data in the same marine area.

The analysis of the wind effect on the NO_2 spatial distribution around Helsinki allowed the estimation of the emission coefficient and lifetime. The method developed for megacities demonstrated its applicability also to Helsinki and its surrounding urban area (about 1 million inhabitants). Thus, in principle, the same methodology could be applied to similar small-scale cities elsewhere. Furthermore, it can be noted that sorting the data according to the wind speed and direction, as described in this paper, is a very useful tool for many different applications of satellite data.

The good agreement with the NO_x emission data confirmed that OMI NO_2 data can be used to detect the signal coming from the ship emissions also in a busy area like the Baltic Sea, where the effect of coastal pollution sources can mix with the emission coming from the ships to the marine boundary layer. OMI NO_2 tropospheric columns reproduce the same year-to-year variability shown by the emissions derived from the model calculation. In particular, both the emission data and the OMI observations showed the drop in year 2009, corresponding to the economical crisis. This confirmed the results obtained for other regions in previous works (e.g., de Ruyter de Wildt et al., 2012).

This paper demonstrated that satellite data contribute significantly to monitoring the pollution levels and environmental changes at high latitude and over sea, where atmo-

ACPD
14, 2021–2042, 2014

spheric concentration information as given by satellite instruments are sparsely available from other sources. Monitoring the NO_2 levels from satellite in the Baltic Sea area remains challenging for many reasons: the interested area is dark for much of the year. Using for example Sun-synchronous satellite, as done in this work, and allowing only solar zenith angle smaller than 70° to reduce the uncertainties, implies that no data are available from November to February over northern Europe. This highlights also the need to develop satellite-based instruments with particular focus on the Arctic region, in order to monitor both land and marine air quality at high latitudes, i.e. with several satellite overpass in one day. In this sense, the NO_2 retrieval should be in future improved and optimized for situations with high solar zenith angle and high albedo (as for snow/ice covered surfaces).

Furthermore, the signal coming from the ships and from Baltic coastal area is relatively small compared to other more polluted regions. This makes the detection even more difficult, because the signal is close to the instrumental detection limit. In addition, the Baltic Sea area is relatively small and the sources of emission are close to each other; this increases the difficulty in identifying the signal coming from different sources. Nevertheless, the method applied in this study allows to distinguish relatively close and small sources, averaging over many days over a grid box smaller than the instrument pixel size and increasing the effective spatial resolution.

The results achieved in this work might be improved using data with higher spatial resolution, i.e. smaller pixel size, as they will become available in 2015 from TROPOspheric Monitoring Instrument (TROPOMI), within the ESA/GMES Sentinel 5 Precursor mission. The instrument will provide daily global coverage with a high spatial resolution of $7 \times 7\,km^2$, which will improve the OMI pixel size ($13 \times 24\,km^2$).

Acknowledgements. This work was founded by ESA-SAMBA project on ship emission monitoring in the Baltic Sea area. The Dutch-Finnish-built OMI instrument is part of the NASA EOS Aura satellite payload. The OMI project is managed by KNMI and the Netherlands Agency for Aerospace Programs (NIVR).We acknowledge the NASA Earth Science Division for funding of OMI NO_2 standard product development and archiving.

ACPD
14, 2021–2042, 2014

References

Beirle, S., Platt, U., von Glasow, R., Wenig, M., and Wagner, T.: Estimate of nitrogen oxide emissions from shipping by satellite remote sensing, Geophys. Res. Lett., 31, L18102, doi:10.1029/2004GL020312, 2004. 2023

Beirle, S., Boersma, K. F., Platt, U., Lawrence, M. G., and Wagner, T.: Megacity emissions and lifetimes of nitrogen oxides probed from space, Science, 333, 1737–1739, doi:10.1126/science.1207824, 2011. 2023, 2024, 2026, 2029, 2030

Bechle, M. J., Millet, D. B., and Marshall, J. D.: Remote sensing of exposure to NO_2: satellite versus ground-based measurement in a large urban area, Atmos. Environ., 69, 345–353, doi:10.1016/j.atmosenv.2012.11.046, 2013. 2023

Boersma, K. F., Eskes, H. J., Dirksen, R. J., van der A, R. J., Veefkind, J. P., Stammes, P., Huijnen, V., Kleipool, Q. L., Sneep, M., Claas, J., Leitão, J., Richter, A., Zhou, Y., and Brunner, D.: An improved tropospheric NO_2 column retrieval algorithm for the Ozone Monitoring Instrument, Atmos. Meas. Tech., 4, 1905–1928, doi:10.5194/amt-4-1905-2011, 2011. 2024, 2025

Bucsela, E. J., Krotkov, N. A., Celarier, E. A., Lamsal, L. N., Swartz, W. H., Bhartia, P. K., Boersma, K. F., Veefkind, J. P., Gleason, J. F., and Pickering, K. E.: A new stratospheric and tropospheric NO_2 retrieval algorithm for nadir-viewing satellite instruments: applications to OMI, Atmos. Meas. Tech., 6, 2607–2626, doi:10.5194/amt-6-2607-2013, 2013. 2024, 2025

Castellanos, P., and Boersma, K. F.: Reductions in nitrogen oxides over Europe driven by environmental policy and economic recession, Sci. Rep., 2, 265; doi:10.1038/srep00265, 2012. 2023, 2028

Corbett, J. J., Winebrake, J. J., Green, E. H., Kasibhatla, P., Eyring, V., and Lauer, A.: Mortality from ship emissions: a global assessment, Environ. Sci. Technol., 41, 8512–8518, 2007. 2024

David, L. M. and Nair, P. R.: Tropospheric column O_3 and NO_2 over the Indian region observed by Ozone Monitoring Instrument (OMI): seasonal changes and long-term trends, Atmos. Environ., 65, 25–39, doi:10.1016/j.atmosenv.2012.09.033, 2013. 2023

de Ruyter de Wildt, M., Eskes, H., and Boersma, K. F.: The global economic cycle and satellite-derived NO_2 trends over shipping lanes, Geophys. Res., Lett., 39, L01802, doi:10.1029/2011GL049541, 2012. 2023, 2024, 2028, 2032

ACPD
14, 2021–2042, 2014

Eyring, V., Isaksen, I. S. A., Berntsen, T., Collins, W. J., Corbett, J. J., Endresen, O., Grainger, R. G., Moldanova, J., Schlager, H., and Stevenson, D. S.: Transport impacts on atmosphere and climate: shipping, Atmos. Environ., 44, 4735–4771, doi:10.1016/j.atmosenv.2009.04.059, 2010. 2024

Fioletov, V. E., McLinden, C. A., Krotkov, N., Moran, M. D., and Yang, K.: Estimation of SO_2 emissions using OMI retrievals, Geophys. Res. Lett., 38, L21811, doi:10.1029/2011GL049402, 2011. 2025

Franke, K., Richter, A., Bovensmann, H., Eyring, V., Jockel, P., Hoor, P., and Burrows, J. P.: Ship emitted NO_2 Franke, K., Richter, A., Bovensmann, H., Eyring, V., Jöckel, P., Hoor, P., and Burrows, J. P.: Ship emitted NO_2 in the Indian Ocean: comparison of model results with satellite data, Atmos. Chem. Phys., 9, 7289–7301, doi:10.5194/acp-9-7289-2009, 2009. 2023

Ghude, S. D., Kulkarni, S. H., Jena, C., Pfister, G. G., Beig, G., Fadnavis, S., and van der A, R. J.: Application of satellite observations for identifying regions of dominant sources of nitrogen oxides over the Indian Subcontinent, J. Geophys. Res., 118, 1075–1089, doi:10.1029/2012JD017811, 2013. 2023

Haario, H., Saksman, E., and Tamminen, J.: An adaptive Metropolis algorithm, Bernoulli, 7, 223–242, 2001. 2027

Haario, H., Laine, M., Mira, A., and Saksman, E.: DRAM: Efficient adaptive MCMC, Stat. Comput., 16, 339–354, 2006. 2027

Hilboll, A., Richter, A., and Burrows, J. P.: Long-term changes of tropospheric NO_2 over megacities derived from multiple satellite instruments, Atmos. Chem. Phys., 13, 4145–4169, doi:10.5194/acp-13-4145-2013, 2013. 2023

Jalkanen, J.-P., Brink, A., Kalli, J., Pettersson, H., Kukkonen, J., and Stipa, T.: A modelling system for the exhaust emissions of marine traffic and its application in the Baltic Sea area, Atmos. Chem. Phys., 9, 9209–9223, doi:10.5194/acp-9-9209-2009, 2009. 2027

Jalkanen, J.-P., Johansson, L., Kukkonen, J., Brink, A., Kalli, J., and Stipa, T.: Extension of an assessment model of ship traffic exhaust emissions for particulate matter and carbon monoxide, Atmos. Chem. Phys., 12, 2641–2659, doi:10.5194/acp-12-2641-2012, 2012. 2027, 2031

Laine, M.: Adaptive MCMC Methods with Applications in Environmental and Geophysical Models, Finnish Meteorological Institute Contributions, No. 69, available at: http://urn.fi/URN:ISBN:978-951-697-662-7 (last access: 22 January 2014), 2008. 2027

ACPD
14, 2021–2042, 2014

Lamsal, L. N., Martin, R. V., Parrish, D. D., and Krotkov, N. A.: Scaling relationship for NO_2 pollution and urban population size: a satellite perspective, Environ. Sci. Technol., 47, 7855–7861, doi:10.1021/es400744g, 2013. 2023

Marmer, E., Dentener, F., Aardenne, J. v., Cavalli, F., Vignati, E., Velchev, K., Hjorth, J., Boersma, F., Vinken, G., Mihalopoulos, N., and Raes, F.: What can we learn about ship emission inventories from measurements of air pollutants over the Mediterranean Sea?, Atmos. Chem. Phys., 9, 6815–6831, doi:10.5194/acp-9-6815-2009, 2009. 2023

Richter, A., Eyring, V., Burrows, J., Bovensmann, H., Lauer, A., Sierk, B., and Crutzen, P.: Satellite measurements of NO_2 from international shipping emissions, Geophys. Res. Lett., 31, L23110, doi:10.1029/2004GL020822, 2004. 2023

Russell, A. R., Valin, L. C., and Cohen, R. C.: Trends in OMI NO_2 observations over the United States: effects of emission control technology and the economic recession, Atmos. Chem. Phys., 12, 12197–12209, doi:10.5194/acp-12-12197-2012, 2012. 2023

Stavrakou, T., Müller, J.-F., Boersma, K. F., van der A, R. J., Kurokawa, J., Ohara, T., and Zhang, Q.: Key chemical NO_x sink uncertainties and how they influence top-down emissions of nitrogen oxides, Atmos. Chem. Phys., 13, 9057–9082, doi:10.5194/acp-13-9057-2013, 2013. 2025

Streets, D. G., Canty, T., Carmichael, G. R., de Foy, B., Dickerson, R. R., Duncan, B. N., Edwards, D. P., Haynes, J. A., Henze, D. K., Houyoux, M. R., Jacob, D. J., Krotkov, N. A., Lamsal, L. N., Liu, Y., Lu, Z., Martin, R. V., Pfister, G. G., Pinder, R. W., Salawitch, R. J., and Wecht, K. J.: Emissions estimation from satellite retrievals: a review of current capability, Atmos. Environ., 77, 1011–1042, 2013. 2023

van der A, R. J., Eskes, H. J., Boersma, K. F., van Noije, T. P. C., Van Roozendael, M., DeSmedt, I., Peters, D. H. M. U., and Meijer, E. W.: Trends, seasonal variability and dominant NO_x source derived from a ten year record of NO_2 measured from space, J. Geophys. Res., 113, D04302, doi:10.1029/2007JD009021, 2008. 2023

Vinken, G. C. M., Boersma, K. F., van Donkelaar, A., and Zhang, L.: Constraints on ship NO_x emissions in Europe using GEOS-Chem and OMI satellite NO_2 observations, Atmos. Chem. Phys. Discuss., 13, 19351–19388, doi:10.5194/acpd-13-19351-2013, 2013. 2023

ACPD
14, 2021–2042, 2014

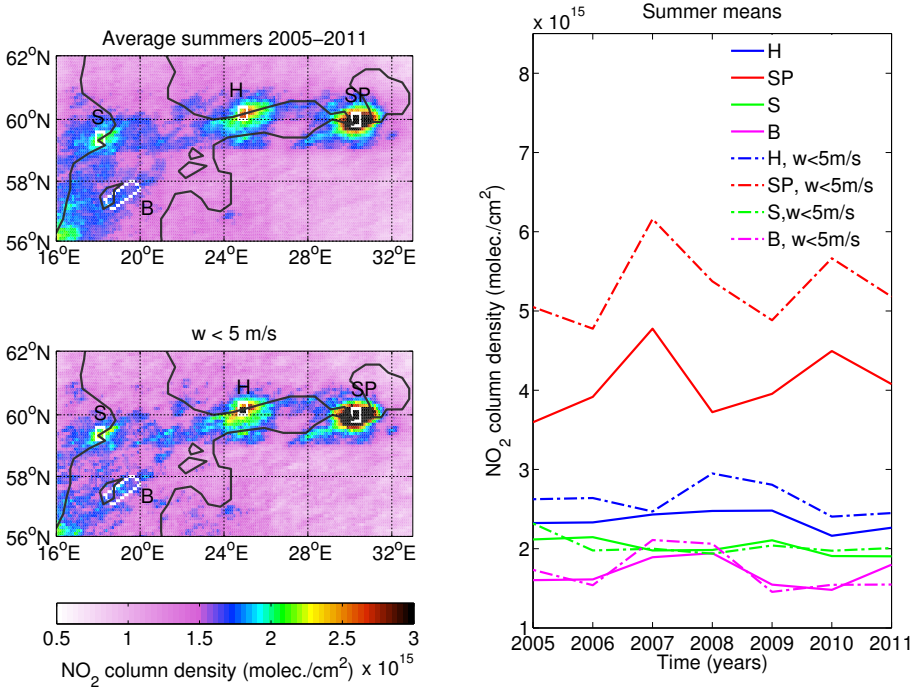

Fig. 1. OMI tropospheric NO_2 column averaged over the summer days in 2005–2011, under all wind and weak wind conditions (upper and lower left panel, respectively). The main coastal cities and the selected area in the Baltic Sea region are marked with their initials: Helsinki (H, 60.2° N, 25.0° E), Stockholm (S, 59.3° N, 18.0° E), Saint Petersburg (SP, 59.95° N, 30.3° E) and Baltic Sea (B, 57.5° N, 19° E). The right panel illustrates the time series of the seasonal means of NO_2 for these locations. The grid pixels included in the summer means are marked by the white boxes in the left panels.

ACPD
14, 2021–2042, 2014

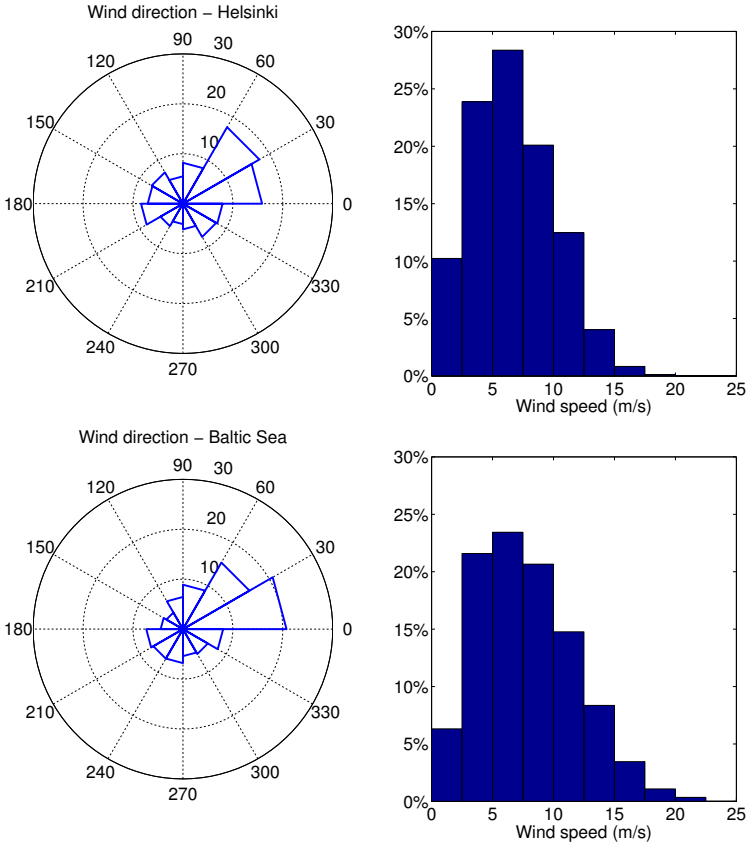

Fig. 2. Wind directions (left panels) and wind speed histogram (right panels) averaged below 950 hPa level over all summers 2005–2011. The azimuthal angle 0 corresponds to wind from West to East (according to the ECMWF definition). Both the data from Helsinki and Baltic Sea areas, as defined by the white boxes in Fig. 1, are presented in the upper and lower panels, respectively.

ACPD
14, 2021–2042, 2014

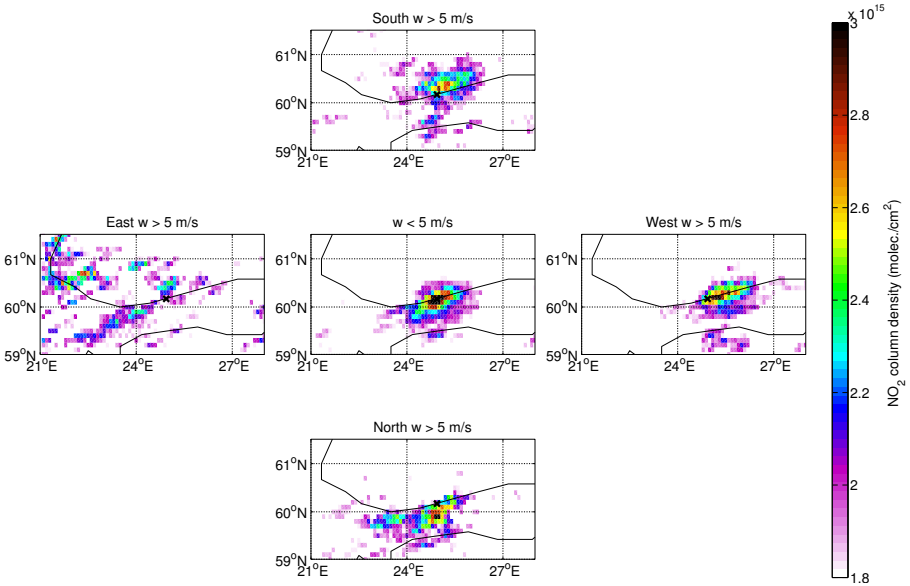

Fig. 3. Summer 2005–2011 mean tropospheric NO_2 columns around Helsinki (black cross) for different wind conditions, i.e., weak wind (center panel) and four main wind direction sectors (surrounding panels). NO_2 maps for winds blowing from North, West, South and East, are respectively showed moving clockwise from the top panel.

ACPD
14, 2021–2042, 2014

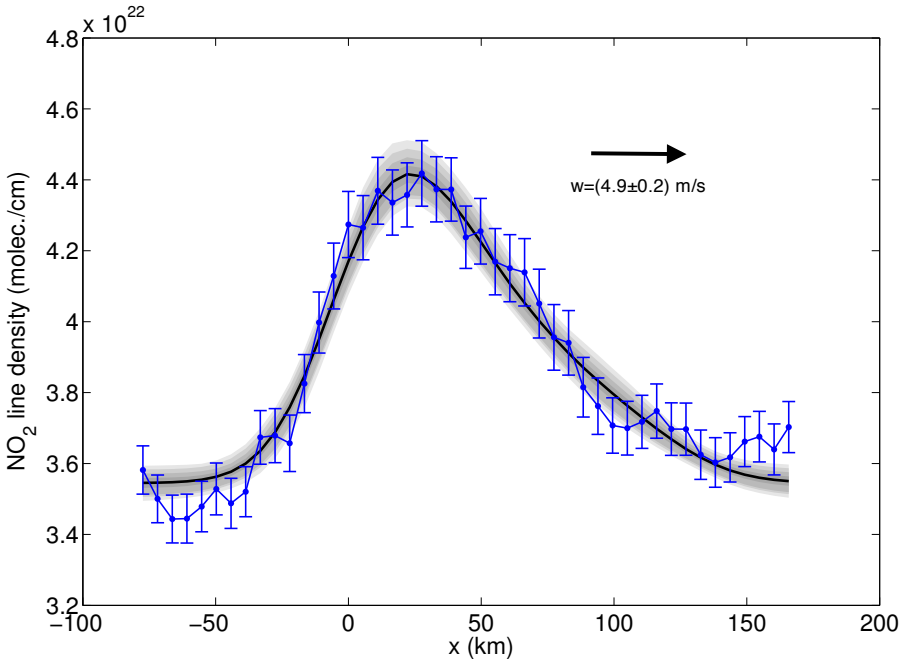

Fig. 4. OMI NO_2 line density (blue color) integrated in the zonal direction (i.e. with respect to latitude) for westerly wind conditions as a function of the distance (x) to Helsinki. Positive number in x axis indicates the East direction. The error bars were derived using the error propagation for the discrete integral. The black line shows the MCMC fitted model and the grey areas correspond to the 50–99 % probability uncertainty regions.

ACPD
14, 2021–2042, 2014

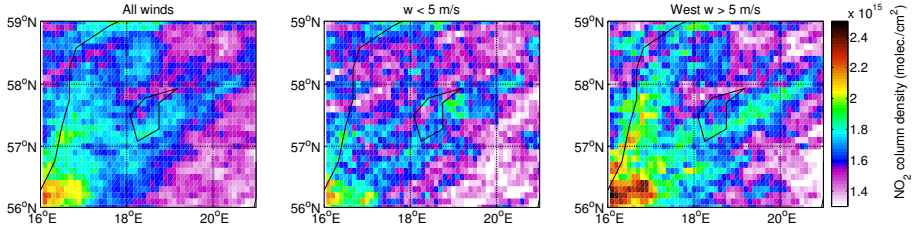

Fig. 5. Summer 2005–2011 mean tropospheric NO_2 columns in the Baltic Sea for all wind conditions (first panel), weak winds, i.e. $w < 5\,m\,s^{-1}$ (central panel) and westerly winds with $w > 5\,m\,s^{-1}$ (right panel).

ACPD
14, 2021–2042, 2014

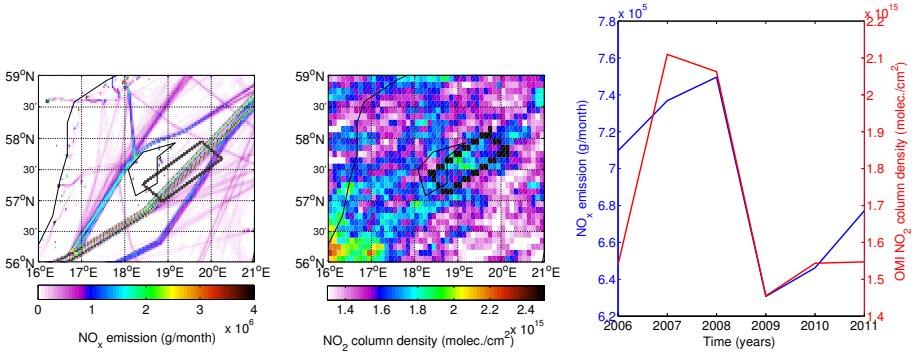

Fig. 6. Comparison between STEAM NO_x emissions and OMI NO_2 tropospheric columns during the period 2006–2011. Left panel: July–August cumulative NO_x emissions from STEAM model; central panel: July–August mean NO_2 tropospheric columns from OMI; right panel: time series of both NO_x emissions (blue line) and NO_2 columns (red line) as derived from the mean value within the black boxes in the left and central panel, respectively.

ACPD
14, 2021–2042, 2014